Geometrical percolation threshold of overlapping ellipsoids

E. J. Garboczi,[1] K. A. Snyder,[1] and J. F. Douglas[2]
[1]*Building Materials Division, National Institute of Standards and Technology, Gaithersburg, Maryland 20899*
[2]*Polymers Division, National Institute of Standards and Technology, Gaithersburg, Maryland 20899*

M. F. Thorpe
Department of Physics and Astronomy and Center for Fundamental Materials Research, Michigan State University, East Lansing, Michigan 48824
(Received 18 January 1995)

A recurrent problem in materials science is the prediction of the percolation threshold of suspensions and composites containing complex-shaped constituents. We consider an idealized material built up from freely overlapping objects randomly placed in a matrix, and numerically compute the geometrical percolation threshold p_c where the objects first form a continuous phase. Ellipsoids of revolution, ranging from the extreme oblate limit of platelike particles to the extreme prolate limit of needlelike particles, are used to study the influence of object shape on the value of p_c. The reciprocal threshold $1/p_c$ (p_c equals the critical volume fraction occupied by the overlapping ellipsoids) is found to scale linearly with the ratio of the larger ellipsoid dimension to the smaller dimension in both the needle and plate limits. Ratios of the estimates of p_c are taken with other important functionals of object shape (surface area, mean radius of curvature, radius of gyration, electrostatic capacity, excluded volume, and intrinsic conductivity) in an attempt to obtain a universal description of p_c. Unfortunately, none of the possibilities considered proves to be invariant over the entire shape range, so that p_c appears to be a rather unique functional of object shape. It is conjectured, based on the numerical evidence, that $1/p_c$ is minimal for a sphere of all objects having a finite volume.

PACS number(s): 82.70.Kj, 64.60.Ak, 81.35.+k

I. INTRODUCTION

An important problem in describing the transport properties of random multiphase materials is the prediction of percolation thresholds as a function of volume fraction [1,2], interparticle interaction [3], shape [4–8], and orientation of the component phases or particles of the random material [9]. In many practical applications, the structure of composite materials evolves in time by chemical reaction so that the percolation transition occurs after an "ageing time" (e.g., cement-based materials, gels) [10–16]. These applications motivate further study of ordinary geometrical percolation theory, which provides insights into these kinds of complex kinetic processes.

An idealized model of percolation is that of completely permeable objects, whose free overlap as more and more objects are randomly added to a matrix eventually results in a geometrically connected phase. There are important materials science applications of this idealized model. For example, we could imagine a material that develops multiple cracks, which eventually percolate geometrically. Since cracks can interpenetrate, the percolation model of randomly overlapping objects is physically appropriate. A second example is the random growth of a microstructure such that an isolated phase becomes geometrically continuous or a continuous phase becomes geometrically isolated. Particular realizations of this random growth include the disconnection of the pore phase in sintering ceramic powders and hydrating cement-based materials [15,17], and the liquid-to-solid transition in sol-gel materials and cement-based materials [10,15]. The gradual buildup of a connected phase via overlap of permeable particles, although idealized, is similar to these examples of chemical growth in real materials.

Ideas from percolation theory are commonly applied to the properties of suspensions and composites of impenetrable particles, where a "percolation threshold" is identified with the asymptotic variation of some material property P near a characteristic concentration ϕ^*,

$$P \sim |\phi^* - \phi|^{-\delta} , \tag{1}$$

where ϕ is the volume fraction of the suspended "particles" and δ is a "critical exponent" describing the often rapid variation of P near the threshold concentration ϕ^*. Although this phenomenological approach to describing the properties P of complex random materials is often successful in summarizing experimental observations, the identification of the percolation threshold ϕ^*, obtained by fitting experimental data to Eq. (1), with the geometrical threshold p_c should be made with caution. Even in the well-understood case of the conductivity of a suspension of particles [18,19], there is only a simple relation between the apparent percolation threshold ϕ^* and p_c in the limit where the suspended particles have conductivities extremely different from the suspending medium. Otherwise, when the ratio of the particle and medium conductivities is not as large, the experimental estimate ϕ^* for the conductivity percolation threshold can differ

from the geometrical quantity p_c. The use of Eq. (1) for other properties where theory is more limited, is evidently even more suspect, but the practical utility of this approach is undeniable. These concentration thresholds are often reported in the physical literature and the estimation of these parameters is a matter of practical interest.

Equation (1) is often used to successfully describe the electrical and thermal conductivity [6,20–22], dielectric constant [23], and shear modulus [5] of composites, the permeability of porous media [24], and transport properties, such as the viscosity of fluid suspensions of rigid particles [25–27]. It is known that ϕ^* varies significantly with particle asymmetry [25,26] and qualitatively similar variations of ϕ^* with shape are found for these various transport properties. This phenomenology suggests that the dependence of p_c on particle shape should give some insight into observed variations of ϕ^*. This possibility remains to be checked through more quantitative comparisons between ϕ^* and p_c obtained from numerical calculations where the mixture geometry is precisely specified.

In the present paper, we compute the geometrical percolation threshold p_c in a model-two-phase material in which objects are randomly placed without regard to overlap. The value of p_c is defined by a transition in the *connectivity* of the randomly placed objects from a disconnected to a connected state. In general, p_c is much easier to compute than ϕ^* since determination of the quantities in Eq. (1) requires a full solution of the appropriate hydrodynamic equations (Laplace, Navier-Stokes, etc.) for a very complicated geometry and general boundary conditions.

There have been many previous efforts to obtain the variation of p_c with particle asymmetry [28–38]. Significant progress especially has been made in two dimensions where a fairly general understanding of p_c in terms of the leading order virial coefficient for the electrical conductivity has been obtained for overlapping elliptical particles and particles of a more general shape [29]. Results in three dimensions (3D) are more fragmentary. The present paper is intended to fill this gap by performing numerical computations of p_c over a wide range of aspect ratios, from the extreme oblate limit to the extreme prolate limit.

To obtain further insight into the shape dependence of p_c for nonspherical particles we follow the previous successful 2D approach [29] and theoretical arguments by Balberg [28] and others that attempt to relate p_c to other more analytically and numerically tractable measures of object shape. Balberg [38], for example, has derived rough bounds of p_c for different objects in terms of the "excluded volume" between different objects. From this work and the well-known contribution of Scher and Zallen [39], which phenomenologically relates the on-lattice and off-lattice site percolation thresholds of nonoverlapping spherical particles, we seek an "invariant" ratio of p_c and other particle properties of the ellipsoid that universally summarizes the shape dependence of p_c for ellipsoids and ultimately for particles having more general shapes. We approach this goal by calculating explicitly a large range of functionals of particle shape for ellipsoids (surface area, mean radius of curvature, radius of gyration, electrostatic capacity, excluded volume, and intrinsic conductivity) and forming ratios with p_c.

In Sec. II, we begin our investigation with a review of important functionals of particle shape and explicit analytic results for ellipsoidal particles that are scattered throughout the mathematical and physical literature. Section III develops a rough perturbative estimate of the percolation threshold ϕ^* for the conductivity and reviews past efforts to describe the shape dependence of p_c through shape functionals. We proceed to the numerical determination of p_c for ellipsoids and a brief description of the algorithm used in Sec. IV. Numerical results for p_c are given separately in Sec. V and fitted by a Padé-type approximant. We finally return to a discussion of these numerical results in terms of shape functionals.

II. BASIC FUNCTIONALS OF OBJECT SHAPE AND THEIR EVALUATION FOR ELLIPSOIDS OF REVOLUTION

Shape functionals play a large role in many physical applications [40–42], and have been subject to extensive mathematical investigation [40]. In the present paper, these functionals of particle shape are normalized so as to be independent of the size of the particle and to equal unity for a sphere. The shape functionals considered in this paper include the following: the surface area, the mean radius of curvature, the radius of gyration, the electrostatic capacity, the excluded volume (binary cluster integral for purely repulsive particles in the theory of nonideal gases), and the intrinsic conductivity for both insulating and superconducting objects in a normal conducting matrix. For ellipsoids of revolution, these are all given by simple analytic formulas. To make these shape functionals equal to unity for a sphere and independent of absolute particle size, we normalize them by the same property defined for a sphere with equal volume to the ellipsoid, i.e., $V_{\rm sph}=(4\pi/3)r^3=(4\pi/3)ab^2$, where a is the length of the symmetry axis, b is the length of each axis perpendicular to the symmetry axis, and a/b is the aspect ratio of the ellipsoid.

A striking qualitative feature of the shape functionals we investigate are the general "isoperimetric relations" [40] that show that these functionals tend to be minimized for objects having more symmetric shapes, with absolute minima existing for the sphere, the most symmetric object having a finite volume. The explicit illustration of these famous isoperimetric inequalities for ellipsoidal particles and for a variety of properties should have independent interest for the insight it provides into the interrelation between important particle properties.

A. Surface area

The surface area of an ellipsoid of revolution is well known [43]. Normalized by the surface area of a sphere with equal volume, the surface area A becomes

$$A=\begin{cases}\frac{1}{2}\left[\frac{a}{b}\right]^{1/3}\left[\sqrt{1-\epsilon^2}+\frac{\sin^{-1}(\epsilon)}{\epsilon}\right], & \epsilon^2=1-\left[\frac{b}{a}\right]^2 \text{ (prolate)} \quad (2)\\ \frac{1}{2}\left[\frac{b}{a}\right]^{2/3}\left[1+\frac{(1-\epsilon^2)}{2\epsilon}\ln\left[\frac{1+\epsilon}{1-\epsilon}\right]\right] & \epsilon^2=1-\left[\frac{a}{b}\right]^2 \text{ (oblate) .} \quad (3)\end{cases}$$

The surface area of a triaxial ellipsoid involves a more complicated closed form involving elliptic functions [44,45]. It is a classical result from mathematical antiquity that of all objects of a given volume, the sphere has the minimum surface area and that in 2D, of all regions of finite area, the circle has the minimum perimeter [40]. Such inequalities for general shape functionals have then come to be called "isoperimetric." The reciprocal of the quantities defined in Eq. (2) and (3) are also widely known as the "sphericity" of a particle [46–48].

B. Mean radius of curvature

The mean radius of curvature of an object is just the average radius of the local surface curvature, integrated over the entire surface. Normalized by the radius of a sphere with equal volume (the mean radius of curvature of a sphere is just the spherical radius), the mean radius of curvature R for an ellipsoid of revolution becomes [43],

$$R=\begin{cases}\frac{1}{2}\left[\frac{a}{b}\right]^{2/3}\left[1+\frac{(1-\epsilon^2)}{2\epsilon}\ln\left[\frac{1+\epsilon}{1-\epsilon}\right]\right], & \epsilon^2=1-\left[\frac{b}{a}\right]^2 \text{ (prolate)} \quad (4)\\ \frac{1}{2}\left[\frac{b}{a}\right]^{1/3}\left[\sqrt{1-\epsilon^2}+\frac{\sin^{-1}(\epsilon)}{\epsilon}\right], & \epsilon^2=1-\left[\frac{a}{b}\right]^2 \text{ (oblate) .} \quad (5)\end{cases}$$

The value of R for the triaxial ellipsoid has also been worked out [49].

C. Radius of gyration

The radius of gyration R_g of a triaxial ellipsoid is simply [50]

$$R_g^2=\tfrac{1}{5}[a^2+b^2+c^2] , \quad (6)$$

where a,b,c are the three semiaxis lengths. Calculating R_g for an ellipsoid of revolution, $c=b$, and normalizing by R_g for the sphere of equal volume gives

$$R_g^2=\frac{1}{3}\left[\left[\frac{a}{b}\right]^{4/3}+2\left[\frac{b}{a}\right]^{2/3}\right] . \quad (7)$$

D. Electrostatic capacity

The electrostatic capacity of an object is defined by the following problem. Assume the object is conducting and charged so that the surface has a constant (unit) potential and the potential outside the object decays to zero at infinite distance. The capacity can then be defined in terms of the asymptotic decay at large distances of the solution to Laplace's equation in the space surrounding the object [40–42]. Units are chosen such that a sphere of radius R has a capacitance $C=R$ [51]. The problem of the capacitance of an ellipsoid of revolution has also been solved [52]. Normalized by the capacitance of a sphere with equal volume, the capacitance of an ellipsoid of revolution equals

$$C=\begin{cases}\frac{x^{-1/3}\sqrt{x^2-1}}{\ln[x+\sqrt{x^2-1}]} & \text{prolate} \quad (8)\\ \frac{x^{-1/3}\sqrt{1-x^2}}{\sin^{-1}[\sqrt{1-x^2}]} & \text{oblate ,} \quad (9)\end{cases}$$

where the aspect ratio $x=a/b$. Hubbard and Douglas [51] have recently shown that the Stokes friction of a Brownian particle is proportional to C to a very good approximation, and that capacity is related to many physical processes and properties relating to the origin of Laplace's equation in describing heat, electrical, and fluid flow [40–42]. This relation between the translational friction and capacity is exact for ellipsoids [51]. It is rigorously known that C is a minimum for a sphere for all objects having a finite volume [40].

E. Excluded volume

The excluded volume for a given object is defined as that volume surrounding and including a given object, which is excluded to another object [53,54]. A similar definition of the excluded area holds in 2D. This functional is always defined for a pair of objects. The "excluded volume" terminology comes from the statistical mechanics of gases, where this functional arises in the leading order concentration expansion (virial expansion) for the pressure in the case of gas particles that repel each other with a hard-core volume exclusion [43].

Isihara [43] gives a general expression for the excluded volume of two convex objects, involving the surface area

and mean radius of curvature of each, and then derives the explicit formula for ellipsoids of revolution. The elegant and general form for $\langle V_{ex} \rangle$ for two convex objects, denoted 1 and 2, is expressed in terms of their surface areas F_i, the average radii of curvature on their surfaces R_i, and their individual volumes V_i. For convex objects the general formula is

$$\langle V_{ex} \rangle = V_1 + V_2 + (A_1 R_1 + A_2 R_2)/4\pi \ . \tag{10}$$

Isihara [43] has proven that a sphere minimizes the excluded volume of all convex bodies of finite volume. One should note that when the two particles are identical, as below, the usual convention is to use one half the quantity shown in Eq. (10). Balberg does not normalize by this factor of one half in his definition of the excluded volume $\langle V_{ex} \rangle$ [28,38]. The excluded volume for ellipsoids of revolution is then obtained by inserting the expressions for A and R, from Eqs. (2)–(5). The value of $\langle V_{ex} \rangle$ normalized by the excluded volume for a sphere with equal volume is invariant to this factor of $\frac{1}{2}$ and results in the final expression for ellipsoids of revolution:

$$\langle V_{ex} \rangle = \frac{1}{4} + \frac{3}{16} z \left[1 + \frac{(1-\epsilon^2)}{2\epsilon} \ln \left[\frac{1+\epsilon}{1-\epsilon} \right] \right] \times \left[\sqrt{1-\epsilon^2} + \frac{\sin^{-1}(\epsilon)}{\epsilon} \right] \tag{11}$$

where $z = a/b$ for prolate ellipsoids, $z = b/a$ for oblate ellipsoids, and $\epsilon^2 = 1 - 1/(z^2)$ [55].

F. Intrinsic conductivity

The conductivity of random two-phase media is a property that has traditionally been associated with percolation phenomena [56]. Exact relations are known between the percolation threshold of the conductivity and p_c [18,19] in limiting situations (see below). The virial expansion for the conductivity can be developed much like the pressure of a nonideal gas in statistical mechanics to yield the expansion in the particle volume fraction ϕ [57],

$$\frac{\sigma_{\text{eff}}}{\sigma_m} = 1 + [\sigma]\phi + O(\phi^2) + \cdots \ , \tag{12}$$

where σ_m is the conductivity of the pure medium without any particles and $[\sigma]$ is defined as the intrinsic conductivity [58]. Two special limits of the intrinsic conductivity are $[\sigma]_\infty$ for superconducting particles and $[\sigma]_0$ for insulating inclusions [58]. The magnitude of these shape functionals is minimized by the sphere for all objects having a finite volume [40,59]. Notably, in 2D, the relation $-[\sigma]_0 = [\sigma]_\infty$ holds for *all* shapes [60], but this relation does not extend to other dimensionalities. In a separate paper [58], we have shown that in 3D, $[\sigma]_\infty$ is proportional (to within 5%) to the intrinsic viscosity (defined similarly to the intrinsic conductivity but for the viscosity of suspensions of rigid particles in a fluid) for a wide range of particle shapes, so that this important shape functional is also implicitly considered in our discussion of $[\sigma]_\infty$ here. In 2D, $[\sigma]_\infty$ is conjectured to equal the intrinsic viscosity [58].

For ellipsoids of revolution, the intrinsic conductivity for superconducting inclusions $[\sigma]_\infty$ is given by

$$[\sigma]_\infty = \frac{1}{9} \frac{1+3L}{L(1-L)} \ , \tag{13}$$

where L is a depolarization factor [61],

$$L = \begin{cases} \left[1 - \frac{1}{\epsilon^2} \right] \left[1 - \frac{1}{2\epsilon} \ln \left[\frac{1+\epsilon}{1-\epsilon} \right] \right], & \epsilon = \sqrt{1-(b/a)^2} \ \text{(prolate)} \quad (14) \\ \frac{1}{\epsilon^2} \left[1 - \frac{\sqrt{1-\epsilon^2}}{\epsilon} \sin^{-1}(\epsilon) \right], & \epsilon = \sqrt{1-(a/b)^2} \ \text{(oblate)} \quad (15) \end{cases}$$

and ϵ is the eccentricity.

The intrinsic conductivity for insulating inclusions $[\sigma]_0$ can be similarly expressed in terms of L,

$$[\sigma]_0 = \frac{2}{9} \frac{(5-3L)}{(1-L^2)} \ . \tag{16}$$

For a sphere, Eqs. (13) and (16) reduce to the well-known results of Maxwell, $[\sigma]_\infty = 3$ and $[\sigma]_0 = -3/2$ [58].

G. Asymptotic limits of shape functionals

In the extreme prolate limit, the aspect ratio a/b diverges, while in the extreme oblate limit, the inverse aspect ratio b/a diverges. In these limits, the above shape functions reduce to the following limiting forms:

$$[\sigma]_\infty \to \begin{cases} \frac{(a/b)^2}{\ln(a/b)} & \text{(prolate)} \\ \frac{b}{a} & \text{(oblate)}, \end{cases} \tag{17}$$

$$-[\sigma]_0 \to \begin{cases} \frac{10}{9} & \text{(prolate)} \\ \frac{4}{9\pi} \frac{b}{a} & \text{(oblate)} \ , \end{cases} \tag{18}$$

$$A \rightarrow \begin{cases} \frac{\pi}{4}\left[\frac{a}{b}\right]^{1/3} & \text{(prolate)} \\ \frac{1}{2}\left[\frac{b}{a}\right]^{2/3} & \text{(oblate)}, \end{cases} \tag{19}$$

$$R \rightarrow \begin{cases} \frac{1}{2}\left[\frac{a}{b}\right]^{2/3} & \text{(prolate)} \\ \frac{\pi}{4}\left[\frac{b}{a}\right]^{1/3} & \text{(oblate)}, \end{cases} \tag{20}$$

$$\langle V_{\text{ex}} \rangle \rightarrow \begin{cases} \frac{3\pi}{32}\frac{a}{b} & \text{(prolate)} \\ \frac{3\pi}{32}\frac{b}{a} & \text{(oblate)}, \end{cases} \tag{21}$$

$$C \rightarrow \begin{cases} \frac{(a/b)^{2/3}}{\ln(a/b)} & \text{(prolate)} \\ \left[\frac{b}{a}\right]^{1/3} & \text{(oblate)}, \end{cases} \tag{22}$$

$$R_g \rightarrow \begin{cases} \frac{1}{\sqrt{3}}\left[\frac{a}{b}\right]^{2/3} & \text{(prolate)} \\ \sqrt{2/3}\left[\frac{b}{a}\right]^{1/3} & \text{(oblate)}. \end{cases} \tag{23}$$

Figure 1 shows a graphical comparison of the shape functionals described in Secs. II A–II F. We observe the widely different variation of these functionals with particle aspect ratio. The very different magnitudes of $[\sigma]_\infty$ and $-[\sigma]_0$ for needlelike particles is especially notable. It is also observed that despite the many differences in the qualitative variation of these functionals with particle asymmetry, all these properties exhibit absolute minima for the sphere. In many of the cases presented, this result has been proved for all objects of finite fixed volume, as was indicated above.

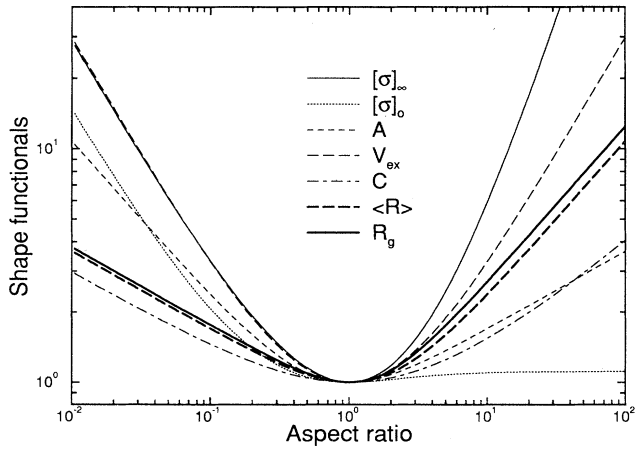

FIG. 1. Various shape functionals (defined in the text) plotted vs aspect ratio for ellipsoids of revolution. Notice that the minimum occurs in each case for the sphere.

III. ESTIMATION OF PERCOLATION THRESHOLDS USING SHAPE FUNCTIONALS

A natural method for obtaining an estimate of the percolation point for conduction problems involving a second phase of randomly inserted objects can be developed by considering the change in the electrical conductivity of a material upon adding a small concentration of objects into the matrix which are "insulating" (much less conducting than the suspending matrix) or "superconducting" (much more conducting than the suspending matrix). The particles are positioned at random locations and with random orientation so that the effective conductivity of the medium σ_{eff} is a scalar that is invariant under rotation of the macroscopic material as a whole. An estimate of the conductive percolation threshold can then be obtained from a simple perturbative criterion [62]. A large variation of the composite conductivity σ_{eff} might be expected when the leading order perturbation in Eq. (12) is on the order of unity,

$$[\sigma]\phi \sim 1 . \tag{24}$$

This perturbative condition [62] defines an order of magnitude estimate of a critical concentration at which the property σ_{eff} should become rapidly varying, indicative of some kind of "perturbation threshold" ϕ^* as was discussed in Sec. I. For perfectly conducting or insulating particles, this critical concentration can be simply identified with a geometrical percolation threshold [18,19].

Previous percolation studies in 2D [29] for elliptical particles and particles of other shapes have indeed shown a nearly shape-independent relation between n_c for geometric percolation and $[\sigma]_\infty$ that is more precise than estimates based on the excluded volume concept. For overlapping objects we recall that the average volume fraction occupied ϕ by objects of general shape is related to the particle volume V_p (or the area A_p in 2D) and the number of particles per unit volume as [29]

$$\phi = 1 - e^{-nV_p} \tag{25}$$

as opposed to impenetrable particles where $\phi = nV_p$. In 2D, it has been shown that the critical number density n_c for geometric percolation times $[\sigma]_\infty$ equals

$$n_c A_p [\sigma]_\infty \approx 2.2 . \tag{26}$$

In the limit of highly anisotropic particles, where $n_c A_p$ is very small, we have $n_c A_p \approx \phi_c$ as in nonoverlapping particles. Equation (26) thus accords qualitatively with expectations from Eq. (24). We note that, recently, the product $A_p[\sigma]_\infty$ has been shown to *exactly* equal [58]

$$A_p[\sigma]_\infty = 2\pi C_L^2 \tag{27}$$

for particles of general shape ($D=2$), where C_L is the "transfinite diameter" or "logarithmic capacity" [58].

The extension of Eq. (24) to 3D is not obvious [63]. Since $[\sigma]_\infty$ and $[\sigma]_0$ generally vary quite differently with

particle anistropy in 3D, as opposed to being equal in magnitude in 2D, we are led to expect different conductivity percolation transitions from Eq. (24) depending on whether the anisotropic particles are insulating or superconducting. Such separate transitions are, in fact, obtained for the transition in conductivity. Consider the example of adding spherical overlapping objects to a conducting matrix. If the spheres are superconducting, the composite conductivity diverges when the spheres percolate at a volume fraction of 0.29 [64]. If the spheres are insulating, the resistivity of the composite diverges at a sphere volume fraction of 0.968, the point at which the matrix becomes disconnected [65].

We also remark that a relation similar to Eq. (24) has been suggested involving $\langle V_{ex} \rangle$ that is applicable to 3D. A virial expansion of the pair connectedness function for overlapping objects naturally leads to the low-density approximation [66] [compare with Eq. (24)]

$$n_c \langle V_{ex} \rangle \approx 1 , \tag{28}$$

which has been predicted to become asymptotically exact in the needle limit [66]. This approximation was introduced heuristically in earlier work by Balberg *et al.* [67]. More recently, Balberg [38] has argued that the constant in Eq. (28) is more generally on the order of unity, and he gives the rough bounds,

$$0.7 < n_c \langle V_{ex} \rangle < 2.8 , \tag{29}$$

which include the estimate of Eq. (28). Evidently, $n_c \langle V_{ex} \rangle$ is not a true invariant, but this ratio does seem to capture the main trends in the dependence of the percolation threshold on particle shape for overlapping particles. In 2D this relation becomes [38]

$$3.2 < n_c \langle A_{ex} \rangle < 4.5 . \tag{30}$$

These shape functionals and bounds on the percolation threshold provide a point of reference for discussing our computations of ψ^c.

IV. PERCOLATION ALGORITHM

In any simulation study of the percolation of randomly placed, overlapping objects, there are three pieces of information that must be known: (1) the position and shape of each object, (2) which, if any, objects overlap each other, and (3) does a connected path composed of overlapping objects exist through the unit cell of the simulation.

The first piece of information, the position and shape of an object, can be stored in several ways. The objects can be stored digitally, in terms of occupied pixels in a digital image [29], which requires a large amount of computer memory, depending, of course, on the resolution with which each shape is represented. A second way, which is used in this simulation study, is, for an Euclidean object, to store the object geometrically, as a set of Cartesian coordinates for the location and orientation of the particle and sufficient numbers to describe the shape [68]. The lengths and orientations of the three semiaxes and the position of its center completely describe a triaxial ellipsoid, for example. In this paper, we consider ellipsoids of revolution, whose shape can also be expressed geometrically. For very oblate or prolate objects in 3D, digital image methods do not have sufficient resolution at the present time, due to computer memory limitations, to give accurate percolation thresholds. We examine the largest range in aspect ratio that is compatible with our computational resources. Periodic boundary conditions were also employed to minimize finite size effects.

The second piece of information that must be known is whether two given objects overlap or touch each other. This is carried out via a contact function. For Euclidean objects, a function can be computed that unambiguously tells if the two objects overlap each other at all, given the centers, orientations, and sizes of the pair of objects. Such a contact function has been worked out for ellipsoids of revolution, for the purposes of carrying out Monte Carlo simulations of hard-core ellipsoid gas problems [69]. Such an algorithm would be very inefficient if every object had to be compared to every other object, so a binning system is used to subdivide the computational cell. To check for overlaps of a given object with other objects then requires only checking the contents of a limited number of bins.

To test the accuracy of our implementation of the contact function described in Ref. [69], we used the algorithm to numerically compute the excluded volume of pairs of identical ellipsoids of various aspect ratios. To do this, we placed a single ellipsoid, oriented along the x axis, in a box, and repeatedly placed a second, identical ellipsoid in the box, with a random center and orientation. Count was kept of those times when the two particles overlapped, as determined numerically by the overlap function. After typically one million trials, the fraction of the trials that resulted in an overlap times the volume of the box was the excluded volume. Figure 2 shows a graph of the numerically determined excluded volume plotted vs the exact excluded volume [see Eq. (11)], for oblate and prolate ellipsoids of revolution. The dashed line is the line of equality.

Finally, overall connectivity must be assessed. Before the objects are percolated, a cluster list is maintained, keeping track of how many distinct clusters of objects exist and which objects are in each cluster. If there are two objects in a cluster, one that touches the top z surface of the computational cell and the other that touches the bottom z surface, then percolation has been achieved. Determination of whether or not an object touches one of the surfaces of the unit cell is carried out using a function that for a given object tells the maximum and minimum x, y, and z points on the object. For a triaxial ellipsoid centered at (x_0,y_0,z_0), with semiaxis lengths a, b, and c, and unit vectors u, v, and w along the a, b, and c axes, respectively, the minimum and maximum x, y, and z points on the surface of the ellipsoid (x_m,y_m,z_m) are given by

$$x_m = x_0 \pm [(au_x)^2 + (bv_x)^2 + (cw_x)^2]^{1/2} , \tag{31}$$

$$y_m = y_0 \pm [(au_y)^2 + (bv_y)^2 + (cw_y)^2]^{1/2} , \tag{32}$$

$$z_m = z_0 \pm [(au_z)^2 + (bv_z)^2 + (cw_z)^2]^{1/2} . \tag{33}$$

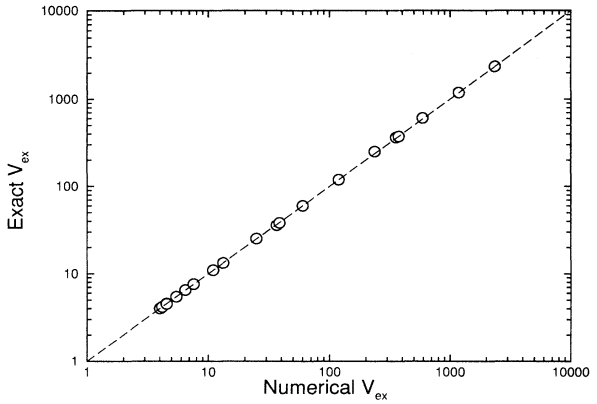

FIG. 2. Comparison between excluded volume, determined numerically, and analytical formula [Eq. (11)] for prolate and oblate ellipsoids of revolution. The dashed line is the line of equality.

V. RESULTS AND DISCUSSION

Table I gives the geometric and percolation data for ellipsoids of revolution whose aspect ratio a/b spanned a range of six orders of magnitude ($1/2000-500$). Each result is the average of at least five realizations, although the number of particles at percolation did not vary more than a few percent between realizations. The number of particles at percolation was recorded (n_c), and the volume fraction of particles at percolation (p_c) was then calculated via Eq. (25). For most of the shapes studied, the actual size of the particle, in relation to the unit edge length periodic computational cell used, was adjusted so that about 20 000 particles were present at percolation. The longest dimension of the particles was kept to less than one tenth of the box size to avoid size scaling problems [70]. For the very prolate particles, this forced the number of particles at percolation to increase sharply, thus practically limiting the computations to a maximum aspect ratio of 500.

TABLE I. Percolation threshold and geometrical data for randomly oriented overlapping ellipsoids of revolution, placed in a cubic cell of unit edge length.

Aspect ratio	a	b	n_c	p_c
1/2000	0.000 012	0.024	22 005	0.000 637
1/1000	0.000 024	0.024	22 028	0.001 275
1/100	0.000 24	0.024	21 691	0.012 48
1/10	0.002 5	0.025	17 089	0.105 8
1/8	0.003 0	0.024	18 637	0.126 2
1/5	0.004 4	0.022	21 659	0.175 7
1/4	0.005 5	0.022	20 046	0.200 3
1/3	0.007 0	0.021	20 103	0.228 9
1/2	0.010	0.020	18 209	0.262 9
3/4	0.015	0.020	13 243	0.283 1
1	0.025	0.025	5 134	0.285 4
3/2	0.030	0.020 0	6 521	0.279 5
2	0.020	0.010 0	36 235	0.261 8
3	0.030	0.010 0	20 219	0.224 4
4	0.040	0.010 0	12 581	0.190 1
5	0.040	0.008 0	16 557	0.162 7
10	0.050	0.005 0	17 389	0.087 03
20	0.060	0.003 0	18 740	0.041 50
30	0.060	0.002 0	26 679	0.026 46
50	0.060	0.001 2	41 827	0.015 02
100	0.060	0.000 6	77 069	0.006 949
200	0.060	0.000 3	141 458	0.003 195
300	0.060	0.000 2	204 373	0.002 052
500	0.060	0.000 12	333 258	0.001 205

Figure 3 shows the inverse of p_c plotted against the aspect ratio a/b. In the extreme oblate limit, it is clear that $1/p_c$ scales linearly in the inverse of the aspect ratio, as can also be seen in Table I. In the extreme prolate limit, $1/p_c$ seems to also scale linearly in the aspect ratio, although it would be necessary to go an order of magnitude further in aspect ratio in order to rule out any small slowly varying nonlinear terms. In these limits, we can write the asymptotic forms approximately as

$$p_c \rightarrow \begin{cases} 0.6\left[\dfrac{b}{a}\right] & \text{(prolate)} \\ 1.27\left[\dfrac{a}{b}\right] & \text{(oblate)} . \end{cases} \tag{34}$$

It is interesting to note that the numerical prefactors differ by close to a factor of 2 in these very different limits. Qualitatively, we observe that $1/p_c$ is minimized for spherical particles. The data strongly suggests a new isoperimetric theorem: Of all objects of a given volume, the sphere has the maximum percolation threshold p_c for overlapping objects.

The solid line in Fig. 3 is a Padé-type approximant,

$$P(x)=\frac{h+fx+gx^{3/2}+cx^2+dx^3}{sx+x^2} , \tag{35}$$

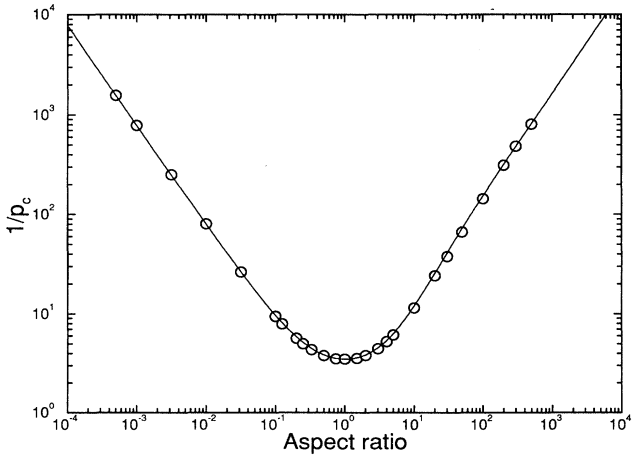

FIG. 3. Inverse of the critical volume fraction for percolation ($1/p_c$) plotted vs aspect ratio of ellipsoids of revolution. The solid line is a Padé-type approximant described in the text. It is fit to both asymptotic limits, the value of $1/p_c$ for the sphere, and is forced to have zero slope at $a/b=1$.

where $x=a/b$, the aspect ratio of the ellipsoids and $P(x)$ is fit to the reciprocal of p_c. Five of the six parameters are fit to the asymptotic behavior of the curve (two slopes, two intercepts) in the extreme prolate and oblate limits, and the known value of $1/p_c$ for the sphere. The sixth parameter is used to force the slope of $P(x)$ to be zero for the sphere ($a/b=1$), since the minimum value of $1/p_c$ was found at this point, and we suspect the above theorem to be true. We call the quantity $P(x)$ a "Padé-type" approximant, since usually Padé approximants only contain integer powers of x [71]. We found that a fractional power was necessary in order to match the data around $a/b=1$. The Padé approximant fits the data extremely well, using the following values: $h=7.742$, $f=14.61$, $g=12.33$, $c=1.763$, $d=1.658$, and $s=9.875$.

After generating the basic percolation data, in light of the perturbative criterion summarized in Eq. (24), it then seems natural to attempt to find some combination of shape functionals that approximates the variation in $1/p_c$. Of course, we ultimately seek a relation that is not restricted to ellipsoidal particles, such as Eq. (26), which appears to hold quite generally in 2D. We search for this relation in terms of finding a shape functional whose product with p_c is a constant, since the value of p_c goes to zero in the oblate and prolate limits, while all the shape functionals displayed in Fig. 1 diverge in these limits, so that the product of the two has a chance of being invariant.

To connect with the extensive work of Balberg and coworkers, we first present a graph of n_c, normalized by $\langle V_{ex} \rangle$ for that particular shape so as to have a dimensionless quantity, vs aspect ratio in Fig. 4. Equation (11) must be multiplied by the appropriate excluded volume for a sphere of equal volume to the ellipsoid using the dimensions for the objects given in Table I. We have also put back in the extra factor of 2 used by Balberg [28,38]. In Fig. 4, it is seen that the normalization with $\langle V_{ex} \rangle$ produces a clear invariant as the extreme oblate limit is approached, and what appears to be a different constant in the extreme prolate limit

$$n_c \langle V_{ex} \rangle \rightarrow \begin{cases} 1.5 & \text{(prolate)} \\ 3.0 & \text{(oblate)} . \end{cases} \tag{36}$$

We note that in the oblate (circular crack) limit, the value of $n_c \langle V_{ex} \rangle$ falls *between* the bounds found by Balberg [38] in Eqs. (29) and (30). Also, the constant in the prolate limit is not equal to unity, as was suggested in Eq. (28). Using Eq. (21) for the asymptotic behavior of $\langle V_{ex} \rangle$, we find that the asymptotic limit of n_c is given by

$$n_c V_p \rightarrow \begin{cases} 5.1 \left[\dfrac{b}{a} \right] & \text{(prolate)} \\ 10.2 \left[\dfrac{a}{b} \right] & \text{(oblate)} . \end{cases} \tag{37}$$

The linear behavior shown in Fig. 3 and Eq. (34) puts restrictions on which shape factors have the potential to form an invariant with the percolation threshold.

Figure 4 also shows the quantity $n_c[\sigma]_\infty$ plotted vs the aspect ratio. This combination, analogous to that used successfully to give an invariant in 2D, clearly fails in 3D for prolate particles. This could have been predicted using the asymptotic relations in Sec. II G.

The results we have obtained in the disc limit disagrees with a previous result of Charlaix [70], who found $n_c \langle V_{ex} \rangle = 1.80$. Using the same normalization of $\langle V_{ex} \rangle$, we find a substantially different value for this product of $n_c \langle V_{ex} \rangle = 3.0$. Our value falls *between* the inequalities found by Balberg [28,38] while Charlaix's result does not. The percolation threshold for discs embedded in a three-dimensional space might intuitively be expected to have properties that span the range between two and three dimensions [58], and this is exactly what our numerical results imply. In Fig. 4, we see that as the ellipsoids change from discs ($a/b \rightarrow 0$) to spheres ($a/b=1$) and then to needles ($a/b \rightarrow \infty$), the value of $n_c \langle V_{ex} \rangle$ changes from 3.0 to 2.7 to 1.5, with 2.8 and below marking the "3D" range found by Balberg [28,38]. Study of Charlaix's computation of n_c does not reveal any obvious mistakes, so we are puzzled by the reason for this disagreement. Figure 4 shows that the variation of $n_c \langle V_{ex} \rangle$ with aspect ratio is very small for all oblate shapes, and since $n_c \langle V_{ex} \rangle = 2.7$ and $p_c = 0.29$ are well known for spheres [64], the estimate $n_c \langle V_{ex} \rangle = 1.8$ appears anomalous.

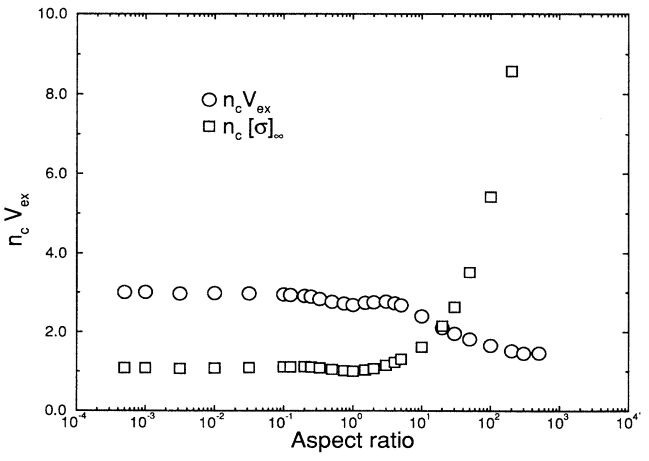

FIG. 4. The critical number density of ellipsoids at percolation normalized by the excluded volume of a single such ellipsoid and by the intrinsic conductivity for superconducting particles, both plotted vs aspect ratio.

Studying the asymptotic limits given in Eq. (17)–(23), we see that there are only four possible choices of shape functions that have the correct or nearly correct prolate and oblate limits: the excluded volume, the radius of gyration R_g times the surface area A, the mean radius of curvature R times the surface area A, and $\Sigma \equiv ([\sigma]_\infty [\sigma]_0)^{1/2}$. All these quantities have the correct asymptotic forms, except that Σ has a square root of the logarithm of the aspect ratio in its denominator in the prolate limit. The $1/p_c$ data, as mentioned above, cannot really rule out such a slight logarithmic dependence in the prolate limit. We have also tried the quantities $p_c[\sigma]_\infty$ and $n_c V_p [\sigma]_\infty$, because of their successful use in

2D [29], but have found that $[\sigma]_\infty$ and $V_p[\sigma]_\infty$ increase much faster than does $1/p_c$ and n_c in the prolate limit. These quantities do work very well, however, in the oblate limit, as can be seen from Eq. (17).

Figure 5 shows the result of multiplying $1/p_c$ by the above shape factors, plotted as a function of aspect ratio. All these quantities do an equally good job of reducing $1/p_c$ to a constant in the prolate and oblate limits, although these constants are different by about a factor of 2, similar to the behavior seen in Fig. 4. Figure 5 clearly shows that the excluded volume does no better than the other shape factors. None of these shape functionals, however, describe the data as well as the Padé approximant shown in Fig. 3.

We, therefore, conclude that the dependence of the percolation threshold, even for the simple case of overlapping identical ellipsoidal objects, cannot be completely described by simple single-particle shape functionals, although the scaling of $1/p_c$ in the extreme prolate and oblate limits can be correctly predicted by several such functions and combinations of functions. It is interesting to note that the intrinsic conductivity for superconducting particles $[\sigma]_\infty$ in 3D fails in scaling p_c or n_c to an invariant, even though it worked extremely well in 2D. The excluded volume, on the other hand, works about the same, to within a factor of 2 or so, in both 2D and 3D. It is hoped that the data in this paper will serve to test new mathematical theories for predicting percolation thresholds based on "microstructural shape" quantities.

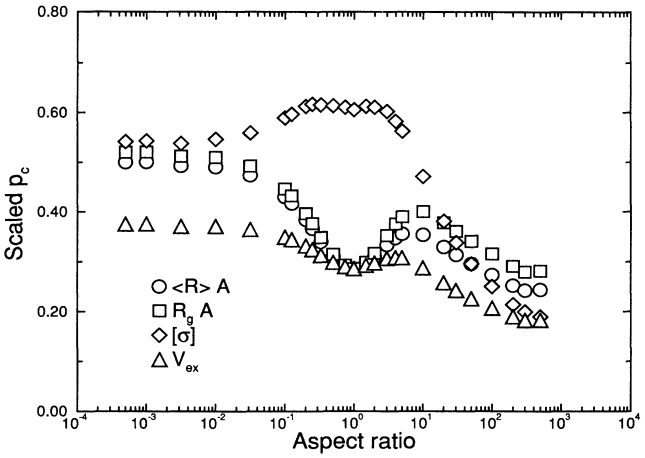

FIG. 5. The critical volume fraction from Fig. 3, normalized by four candidate shape factors that all give the correct scaling with aspect ratio in the extreme oblate and prolate limits, plotted vs aspect ratio.

[1] E. A. Holm and M. J. Cima, J. Am. Ceram. Soc. **72**, 303 (1989).
[2] D. N. Winslow, M. D. Cohen, D. P. Bentz, K. A. Snyder, and E. J. Garboczi, Cem. Concr. Res. **24**, 25 (1994).
[3] A. L. R. Bug, S. A. Safran, G. S. Grest, and I. Webman, Phys. Rev. Lett. **55**, 1896 (1985).
[4] D. M. Bigg, Polym. Eng. Sci. **19**, 1188 (1979), see Ref. [5].
[5] W. Y. Hsu and S. Wu, Polym. Eng. Sci. **33**, 293 (1993).
[6] Y. Wang and M. F. Rubner, Macromolecules **25**, 3284 (1992).
[7] I. Balberg and S. Bozowski, Solid State Commun. **44**, 551 (1982).
[8] K. T. Chung, A. Sabo, and A. P. Pica, J. Appl. Phys. **53**, 6867 (1982).
[9] F. Carmona and A. El Amarti, Phys. Rev. B **35**, 3284 (1987).
[10] B. Gauthier-Manuel, in *Physics of Finely Divided Matter,* edited by N. Boccara and M. Daoud (Springer-Verlag, Berlin, 1985), p. 140.
[11] M. A. V. Axelos and M. Kolb, Phys. Rev. Lett. **64**, 1457 (1990).
[12] M. Tokita, R. Niki, and K. Hikuchi, J. Chem. Phys. **83**, 2583 (1985).
[13] D. F. Hodgson and E. J. Amis, Macromolecules **23**, 2512 (1990).
[14] M. Djabourov, Contemp. Phys. **29**, 273 (1988).
[15] D. P. Bentz and E. J. Garboczi, Cem. Concr. Res. **21**, 325 (1991).
[16] D. M. Bigg, Polym. Eng. Sci. **19**, 1188 (1979).
[17] A. Fizazi, J. Moulton, K. Pakbaz, S. Rughooputh, P. Smith, and A. J. Heeger, Phys. Rev. Lett. **64**, 2180 (1990).
[18] D. J. Bergman, Phys. Rep. **43**, 377 (1978).
[19] D. J. Bergman, in *Macroscopic Properties of Disordered Media,* edited by R. Burridge, S. Childress, and G. Papanicolaou, Lecture Notes in Physics Vol. 154 (Springer-Verlag, Berlin, 1982), p. 10.
[20] B. Abeles, H. L. Pinch, and J. I. Gittleman, Phys. Rev. Lett. **35**, 247 (1975).
[21] P. S. Clarke, J. W. Orton, and A. J. Guest, Phys. Rev. B **18**, 1813 (1978).
[22] W. Y. Hsu and T. Berzins, J. Polym. Sci. **23**, 933 (1985).
[23] W. Y. Hsu, W. G. Holtje, and J. R. Barley, Mater. Sci. Lett. **7**, 459 (1988).
[24] K. Maruyama, K. Okumura, and S. Miyazima, Physica A **191**, 313 (1992).
[25] A. B. Metzner, J. Rheol. **29**, 739 (1985).
[26] T. Kitano, T. Kataoka, and T. Shirota, Rheol. Acta. **20**, 207 (1981).
[27] J. L. Bouillot, C. Camoin, M. Belzons, R. Blanc, and E. Guyon, Adv. Colloid. Interface Sci. **17**, 299 (1982).
[28] I. Balberg, Philos. Mag. B **65**, 991 (1987).
[29] E. J. Garboczi, M. F. Thorpe, M. DeVries, and A. R. Day, Phys. Rev. A **43**, 6473 (1991).
[30] W. Xia and M. F. Thorpe, Phys. Rev. A **38**, 2650 (1988).
[31] T. DeSimone, R. M. Stratt, and S. Demoulini, Phys. Rev. Lett. **56**, 1140 (1086).
[32] E. M. Sevick, P. A. Monson, and J. M. Ottino, Phys. Rev. A **38**, 5376 (1988).
[33] D. Laria and F. Vericat, Phys. Rev. B **40**, 353 (1989).
[34] U. Alon, A. Drory, and I. Balberg, Phys. Rev. A **42**, 4634 (1990).
[35] U. Alon, I. Balberg, and A. Drory, Phys. Rev. Lett. **66**,

2879 (1991).
[36] A. Drory, I. Balberg, U. Alon, and B. Berkowitz, Phys. Rev. A **43**, 6604 (1991).
[37] A. Drory, I. Balberg, and B. Berkowitz, Phys. Rev. E **49**, R949 (1994).
[38] I. Balberg, Phys. Rev. B **31**, 4053 (1985).
[39] H. Scher and R. Zallen, J. Chem. Phys. **53**, 3759 (1970).
[40] G. Pólya and G. Szegö, *Isoperimetric Inequalities in Mathematical Physics: Annals of Mathematical Studies* (Princeton University Press, Princeton, 1951).
[41] J. F. Douglas and A. Friedman, in *Mathematics in Industrial Problems VII: The Institute for Mathematics and Its Applications,* edited by A. Friedman (Springer-Verlag, New York, 1994), Vol. 67, Chap. 15.
[42] J. F. Douglas, H.-X. Zhou, and J. B. Hubbard, Phys. Rev. E **49**, 5319 (1994).
[43] A. Isihara, J. Chem. Phys. **18**, 1446 (1950); Rev. Mod. Phys. **25**, 831 (1953).
[44] S. R. Keller, Math. Comput. **33**, 310 (1979).
[45] P. A. P. Moran, in *Statistics and Probability: Essays in Honor of C. R. Rao,* edited by G. Kallianpur, P. R. Krishnaiah, and J. K. Ghosh (North-Holland, Amsterdam, 1982), pp. 511–518.
[46] H. Wadell, J. Franklin Inst. **217**, 459 (1934).
[47] E. S. Pettyjohn and E. B. Christiansen, Chem. Engr. Prog. **44**, 157 (1948).
[48] S. W. Churchill, *Viscous Flows* (Butterworths, Boston, 1988), Chap. 19.
[49] J. M. Rallison and S. E. Harding, J. Colloid Interface Sci. **103**, 284 (1985).
[50] E. T. Whittaker, *A Treatise on the Analytical Dynamics of Particles and Rigid Bodies* (Dover, New York, 1944), Chap. 5.
[51] J. B. Hubbard and J. F. Douglas, Phys. Rev. E **47**, R2983 (1993).
[52] L. D. Landau and E. M. Lifshitz, *Electrodynamics of Continuous Media* (Pergamon, New York, 1960), p. 24; P. A. Moran, London Math. Soc. Lect. Notes **79**, 192 (1983).
[53] L. Onsager, Ann. NY Acad. Sci. **51**, 627 (1949).
[54] L. A. Santalo, *Integral Geometry and Geometric Probabilities, Encyclopedia of Mathematics, Vol. 1* (Addison Wesley, New York, 1976), p. 282.
[55] A. G. Ogston and D. J. Winsor, J. Phys. Chem. **79**, 2496 (1975).
[56] S. Kirkpatrick, Rev. Mod. Phys. **45**, 574 (1973).
[57] W. F. Brown, J. Chem. Phys. **23**, 1514 (1955).
[58] J. F. Douglas and E. J. Garboczi, Adv. Chem. Phys. **91**, 85 (1995).
[59] M. Schiffer, C. R. Acad. Sci. **244**, 3118 (1957).
[60] J. B. Keller, J. Math. Phys. **5**, 548 (1964); K. S. Mendelson, J. Appl. Phys. **46**, 917 (1975).
[61] J. A. Stratton, *Electromagnetic Theory* (McGraw-Hill, New York, 1941), p. 211.
[62] M. A. Anisimov, S. B. Kiselev, J. V. Sengers, and S. Tang, Physica A **188**, 487 (1992).
[63] An accurate relation between the electrostatic capacity and the bond percolation threshold for $D \geq 3$ lattices has recently been obtained, however [J. F. Douglas and T. Ishinabe, Phys. Rev. E **51**, 1791 (1995)].
[64] M. B. Isichenko, Rev. Mod. Phys. **64**, 961 (1992).
[65] W. T. Elam, A. R. Kerstein, and J. J. Rehr, Phys. Rev. Lett. **52**, 1516 (1984).
[66] A. L. R. Bug, S. A. Safran, and I. Webman, Phys. Rev. Lett. **54**, 1412 (1985).
[67] I. Balberg, C. H. Anderson, S. Alexander, and N. Wagner, Phys. Rev. B **30**, 3933 (1984).
[68] G. E. Pike and C. H. Seager, Phys. Rev. B **10**, 1421 (1974).
[69] J. Vieillard-Baron, J. Chem. Phys. **56**, 4729 (1972), see Appendix B.
[70] E. Charlaix, J. Phys. A **19**, L533 (1986).
[71] C. M. Bender and S. A. Orszag, *Advanced Mathematical Methods for Scientists and Engineers* (McGraw-Hill, New York, 1978).